Procesing '24
37. Međunarodni kongres o procesnoj industriji
29–31. maj 2024, Beograd

Originalni naučni rad
https://doi.org/10.24094/ptk.024.279

KORELACIJA STRUKTURE I POTENCIJALNE FARMAKOLOŠKE AKTIVNOSTI SPIROHIDANTOINA DOBIJENIH IZ α-TETRALONA

CORRELATION OF STRUCTURE AND POTENTIAL PHARMACOLOGICAL ACTIVITY OF SPIROHIDANTOINS DERIVED FROM α-TETRALONE

Anita Lazić*[1], Ivana Đorđević[2], Kristina Gak Simić[1], Luka Matović[1], Aleksandra Mašulović[1], Jelena Lađarević[3], Nemanja Trišović[3],
[1]Univerzitet u Beogradu, Inovacioni centar Tehnološko-metalurškog fakulteta, Beograda
[2]Univerzitet u Beogradu, Institut za hemiju, tehnologiju i metalurgiju, Beograd
[3]Univerztet u Beogradu, Tehnološko-metalurški fakultet, Beograd

Hidantoin je nearomatičan petočlani ciklični ureid koji predstavlja važan strukturni fragment velikog broja farmakološki aktivnih jedinjenja. Derivati ovog petočlanog cikličnog ureida primenjuju se kao antikonvulzivi (fenitoin), antibiotici (nitrofurantoin), antikancerogeni lekovi (enzalutamid) i keratolitici (alantoin). U cilju dizajniranja novih potencijalno farmakološki aktivnih jedinjenja, u ovom radu, sintetisano je šest derivata spirohidantoina koji su u potpunosti strukturno okarakterisani određivanjem temperature topljenja, elementarnom analizom, FT-IR, ^{1}H i ^{13}C NMR spektroskopskim metodama. Efekat supstituenata na pomeranje maksimuma apsorpcije analiziran je primenom linearne korelacije energije solvatacije, dok je uticaj hemijske strukture na farmakološka svojstva derivata spirohidantoina procenjen primenom "pravila broja pet", Veberovog, Eganovog i Gozovog kriterijuma, kao i primenom različitih in silico metoda. U cilju opsežnije analize potencijalne farmakološke aktivnosti sintetisanih spirohidantoina, korelisana su njihova potencijalna farmakološka svojstva sa odgovarajućim efektima rastvarača.

Ključne reči: *derivati imidazolidin-2,4-diona; Kamlet-Taftova jednačina; lipofilnost*

Hydantoin is a nonaromatic five-membered heterocycle, which is considered a valuable, privileged scaffold in medicinal chemistry. The importance of the hydantoin scaffold in drug discovery has been reinforced by several medicines in clinical use, such as anticonvulsants (phenytoin), antibiotics (nitrofurantoin), anticancer drugs (enzalutamide) and keratolytics (allantoin). To design new potentially pharmacologically active compounds, six spirohydantoin derivatives were synthetized and fully characterized by determination of the melting points, elemental analysis, FT-IR, ^{1}H and ^{13}C NMR spectroscopic methods. Effects of the substituents on the shift of the absorption maxima of synthetized compounds were analyzed using the linear solvatation energy relationship, while the influence of the chemical structure on the pharmacokinetically relevant properties of the investigated spirohydantoin derivatives was evaluated using the Lipinski's rule of five, Veber, Egan and Ghose's

* Corresponding author: alazic@tmf.bg.ac.rs
https://orcid.org/0000-0003-4855-3782
Ivana Đorđević: https://orcid.org/0000-0001-5981-9385
Kristina Gak Simić: https://orcid.org/0000-0003-3928-9967
Luka Matović: https://orcid.org/0000-0003-4945-7776
Aleksandra Mašulović: https://orcid.org/0000-0002-5279-7694
Jelena Lađarević: https://orcid.org/0000-0002-5554-7295
Nemanja Trišović: https://orcid.org/0000-0002-9231-4810

empirical criteria, as well as different in silico methods. In order of detailed analysis of the potential pharmacological activity of the synthesized spirohydantoins, their potential pharmacological properties were correlated with the corresponding solvent effects.

Key words: *imidazolidine-2,4-dione derivatives; Kamlet-Taft equation; lipophilicity*

1. Introduction

Currently, there is a frequent explored for pharmacologically active compounds for treatment various disease. The development of more efficient and less toxic compounds often involves the study of new synthetic routes or structural modifications of ongoing compounds and commercially available drugs [1]. The discovery of pharmacological activities of substituted hydantoin derivatives has made amazing progress during the last few decades, and substituted hydantoin derivatives have been therapeutically applied as anticonvulsants (phenytoin), antibiotics (nitrofurantoin), anticancer agents (enzalutamide) and keratolytics (allantoin) [2]. Because of these broad-spectrum pharmacological activities, intensive research efforts have been dedicated in industry and science to the synthesis and structural modifications of hydantoin and its derivatives [3]. Moreover, hydantoin derivatives substituted at positions C-5, N-1 and N-3, alkyl/arylidene spiro, polycyclic, and amino hydantoins have been further investigated with the view of their potential medicinal and pharmaceutical applications [4]. Foregoing investigations indicated that phenol pharmacophore containing compounds have potential anticonvulsant activity along with number of other pharmacological effects. Verma demonstrated that phenytoin derivatives bearing substituted phenoxy acetyl moiety possess potent CNS activities when compared to the standard drug diazepam [5]. Also, Wang showed that 1-methylhydantoin trans-cinnamic imides significantly inhibited the secretion of inflammatory factors (TNF and IL-1) showing good *in vitro* anti-inflammatory activity [6]. Potentially pharmacologically active compounds often bear numerous functional groups capable of forming hydrogen bonds, making them soluble and giving them the ability to form specific interactions with their biomolecular targets. Hydrogen bonding influences the interactions of potentially pharmacologically active organic compounds at different levels of complexity, going from those with other small molecules, up to the highest supramolecular assemblies, e.g., proteins and membranes. These interactions considerably affect the pharmacological activity, pharmacokinetics and physicochemical properties of drugs, hence making hydrogen bonding an important subject of study in drug discovery and development. Therefore, solvatochromic study gives an insight into possible different solute–solvent interactions mimicking the interactions of potentially pharmacologically active organic compounds with their environment [7]. This work describes the synthesis and preliminary spectroscopic characterization of novel bioinspired imidazolidine-2,4-dione derivatives, where the imidazolidine-2,4-dione core was coupled with the bicyclic system on one side and linked to *p*-substituted benzyl group on the other side. Aiming to the hybrid pharmacophore the imidazolidine-2,4-dione moiety was coupled with *p*-substituted benzyl group in our current work and the synthesized compounds were further investigated for their pharmacodynamic and pharmacokinetic benefits [5].

2. Experimental

2.1. General procedure for the synthesis of compounds 1-6

The synthetic route was carried out according to Scheme 1. Starting from commercially available α-tetralone, the modified Bucherer-Bergs reaction was carried out by the use of ammonium carbonate and potassium cyanide to afford the 3',4'-dihydro-2H-spiro[imidazolidine-4,1'-naphthalene]-

2,4-dione [8]. In the following step, alkylation at position 3 of the hydantoin ring was conducted with various *p*-substituted benzyl-chlorides in the presence of K_2CO_3 in *N*,*N*-dimethylformamide (DMF) [9]. Their chemical structure was confirmed by melting points, elemental analysis, FT-IR, NMR and UV–Vis spectroscopic methods.

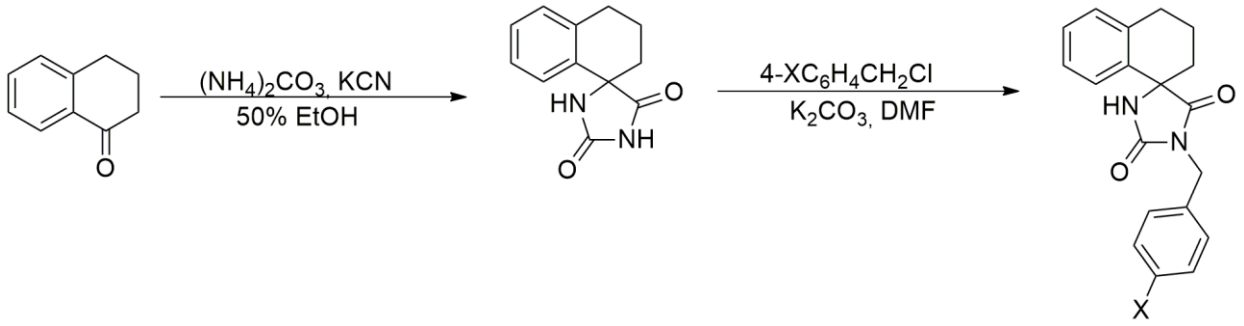

X = H (**1**), CH_3 (**2**), OCH_3 (**3**), Cl (**4**), CN (**5**), NO_2 (**6**)

Scheme 1. Synthetic pathway of the investigated compounds

The melting points were measured on an Electrothermal melting point apparatus without correction. FT-IR spectra of all synthesized compounds were recorded in the range from 400 to 4000 cm^{-1} using a Thermo Scientific Nicolet iS10 spectrometer, within the spectral resolution range 400 to 4000 cm^{-1}. Elemental analysis of the investigated compounds was carried out using microanalyzer Elemental Vario EL III. Absorption spectra were recorded on a Shimadzu 1700 spectrophotometer in solvents of spectroscopic purity (Fluka) at a fixed concentration of 10^{-5} mol dm^{-3}. ^{1}H NMR spectra were recorded on a Bruker Ascend 400 spectrophotometer at 400 MHz, while ^{13}C NMR spectra were recorded at 100 MHz at to the same device. All spectra were recorded at room temperature in deuterated dimethyl sulfoxide (DMSO-d_6). The chemical shifts are expressed in ppm in relation to the reference TMS (δ_H = ppm) in the ^{1}H NMR spectra, that is, the residual signal of the solvent DMSO (δ_C = 39.5 ppm) in the ^{13}C NMR spectra.

3-(Benzyl)-6,7-benzo-1,3-diazaspiro[4.5]decane-2,4-dione (**1**) White crystalline substance: m.p. 126–129 °C, yield: 75 %; IR (KBr, ν/cm^{-1}): 3246, 2931, 1770, 1701, 1603, 1514, 1491, 1438, 1413, 1354, 1340, 1309, 1253, 1202, 1130, 1098, 931, 889, 778, 766, 736, 695. ^{1}H NMR (400 MHz, DMSO-d_6): δ = 8.95 (s, 1H; NH), 7.39–7.36 (m, 2H, Ar(benzyl)-H), 7.32–7.29 (m, 4H, Ar(tetralin)-H), 7.19–7.14 (m, 2H, Ar(benzyl)-H), 6.94 (d, 2H, *J* = 7.6 Hz, Ar(benzyl)-H), 4.63 (s, 2H; N–CH_2), 2.81−2.78 (m, 2H; CH_2), 2.13−2.08 (m, 2H; CH_2), 1.97−1.84 ppm (m, 2H; CH_2); ^{13}C NMR (50 MHz, DMSO-d_6): δ=176.5, 159.1, 156.1, 138.8, 137.4, 129.1, 128.6, 127.3, 127.7, 126.7, 114.4, 62.5, 41.7, 40.7, 39.4, 18.9 ppm; Anal. Calcd. For $C_{19}H_{18}N_2O_2$: C, 74.49, H, 5.92, N, 9.14. Found: C, 74. 46, H, 5.95, N, 9.14.

3-(4-Methylbenzyl)-6,7-benzo-1,3-diazaspiro[4.5]decane-2,4-dione (**2**) White crystalline substance: m.p.153–156 °C, yield: 71 %; IR (KBr, ν/cm^{-1}): 3269, 2945, 2876, 1756, 1703, 1686, 1578, 1514, 1455, 1442, 1410, 1355, 1340, 1289, 1256, 1133, 1117, 1097, 930, 882, 812, 779, 767, 744, 642, 624. ^{1}H NMR (400 MHz, DMSO-d_6): δ = 8.92 (s, 1H; NH), 7.26–7.29 (m, 1H, Ar(benzyl)-H), 7.18–7.14 (m, 6H, Ar(benzyl)-H, Ar(tetralin)-H), 6.92 (d, 1H, *J* = 7.6 Hz, Ar(tetralin)-H), 4.57 (s, 2H; N–CH_2), 2.80−2.77 (m, 2H; CH_2), 2.30 (s, 3H; CH3), 2.13−2.05 (m, 2H; CH_2), 1.95−1.81 ppm (m, 2H; CH_2); ^{13}C NMR (50 MHz, DMSO-d_6): δ=176.4, 156.2, 138.3, 137.1, 129.6, 128.6, 127.8, 126.9, 114.4, 62.4, 41.5, 40.6, 39.4, 28.8, 18.8 ppm; Anal. Calcd. For $C_{20}H_{20}N_2O_2$: C, 74.98, H, 6.29, N, 8.74. Found: C, 74. 96, H, 6.31, N, 8.74.

3-(4-Methoxybenzyl)-6,7-benzo-1,3-diazaspiro[4.5]decane-2,4-dione (**3**) White crystalline substance: m.p. 136–138 °C, yield: 56 %; IR (KBr, ν/cm^{-1}): 3249, 3025, 2951, 1770, 1698, 1615, 1584, 1515, 1495, 1443, 1410, 1356, 1305, 1285, 1252, 1176, 1148, 1125, 1094, 1027, 950, 930, 898, 881, 856, 826, 804, 772, 641, 622, 542, 551, 510, 491, 467, 446, 432. ^{1}H NMR (400 MHz, DMSO-d_6): δ = 8.90 (s, 1H; NH), 7.24 (d, 2H, J = 8.4 Hz, Ar(benzyl)-H), 7.23 (m, 1H, Ar(tetralin)-H), 7.18–7.13 (m, 2H, Ar(tetralin)-H), 6.93 (d, 2H, J = 8.4 Hz, Ar(benzyl)-H), 6.90 (d, 1H, J = 8.0 Hz, Ar(tetralin)-H), 4.55 (s, 2H; N–CH_2), 3.75 (s, 3H; OCH_3), 2.81−2.78 (m, 2H; CH_2), 2.13−2.05 (m, 2H; CH_2), 1.95−1.81 ppm (m, 2H; CH_2); ^{13}C NMR (50 MHz, DMSO-d_6): δ=176.5, 159.1, 156.2, 138.3, 134.5, 129.8, 129.3, 128.6, 127.0, 114.4, 62.4, 55.6, 41.3, 34.0, 28.8, 18.9 ppm. Anal. Calcd. For $C_{20}H_{20}N_2O_3$: C, 71.41, H, 5.99, N, 8.33. Found: C, 71. 36, H, 6.04, N, 8.30.

3-(4-Chlorobenzyl)-6,7-benzo-1,3-diazaspiro[4.5]decane-2,4-dione (**4**) White crystalline substance: m.p.130–133 °C, yield: 82 %; IR (KBr, ν/cm^{-1}): 3232, 3105, 2932, 1767, 1703, 1597, 1490, 1432, 1419, 1350, 1337, 1282, 11154, 1087, 1027, 1015, 951, 943, 816, 761, 742, 619, 510. ^{1}H NMR (400 MHz,DMSO-d_6): δ = 8.90 (s, 1H; NH), 7.24 (d, 2H, J = 8.4 Hz, Ar(benzyl)-H), 7.18–7.13 (m, 2H, Ar(tetralin)-H), 6.93 (d, 2H, J = 8.8 Hz, Ar(benzyl)-H), 6.89 (d, 2H, J = 8.0 Hz, Ar(tetralin)-H), 4.55 (s, 2H; N–CH_2), 2.81−2.78 (m, 2H; CH_2), 2.13−2.05 (m, 2H; CH_2), 1.94−1.81 ppm (m, 2H; CH_2); ^{13}C NMR (50 MHz, DMSO-d_6): δ = 176.5, 159.1, 156.2, 138.3, 134.5, 129.8, 129.4, 128.6, 126.9, 114.4, 62.4, 41.2, 40.6, 39.4, 28.9, 18.9; Anal. Calcd. For $C_{19}H_{17}ClN_2O_2$: C, 66.96, H, 5.03, N, 8.22. Found: C, 66. 94, H, 5.05, N, 8.22.

3-(4-Cyanobenzyl)-6,7-benzo-1,3-diazaspiro[4.5]decane-2,4-dione (**5**) White crystalline substance: m.p. 182–185 °C, yield: 83 %; IR (KBr, ν/cm^{-1}): 3365, 2935, 2865, 2225, 1774, 1708, 1607, 1495, 1437, 1413, 1348, 1340, 1332, 1277, 1111, 1056, 1029, 955, 944, 859, 821, 769, 743, 651, 620, 590. ^{1}H NMR (400 MHz,DMSO-d_6): δ = 9.01 (s, 1H; NH), 7.84 (d, 2H, J = 8.0 Hz, Ar(benzyl)-H), 7.47 (d, 2H, J = 8.0 Hz, Ar(benzyl)-H), 7.25–7.22 (m, 1H, Ar(tetralin)-H), 7.18–7.16(m, 2H, Ar(tetralin)-H), 6.96 (d, 1H, J = 8.4 Hz, Ar(tetralin)-H), 4.70 (s, 2H; N–CH_2), 2.80−2.76 (m, 2H; CH_2), 2.13−2.08 (m, 2H; CH_2), 1.98−1.92 ppm (m, 1H; CH_2), 1.86−1.87 ppm (m, 1H; CH_2); ^{13}C NMR (50 MHz, DMSO-d_6): δ = 176.5, 155.9, 142.8, 138.4, 134.2, 133.1, 129.9, 128.7, 127.0, 119.1, 110.8, 62.6, 41.5, 39.3, 28.8, 18.8 ppm; Anal. Calcd. For $C_{20}H_{17}ClN_3O_2$: C, 72.49, H, 5.17, N, 12.68. Found: C, 72. 51, H, 5.14, N, 12.68.

3-(4-Nitrobenzyl)-6,7-benzo-1,3-diazaspiro[4.5]decane-2,4-dione (**6**) Yellow crystalline substance: m.p. 170–173 °C, yield: 88 %; IR (KBr, ν/cm^{-1}): 3204, 3097, 2933, 2840, 1770, 1708, 1604, 1511, 1439, 1406, 1338, 1288, 1262, 1126, 976, 963, 876, 850, 651. ^{1}H NMR (400 MHz,DMSO-d_6): δ = 9.04 (s, 1H; NH), 8.24 (d, 2H, J = 8.4 Hz, Ar(benzyl)-H), 7.55 (d, 2H, J = 8.8 Hz, Ar(benzyl)-H), 7.25–7.16 (m, 3H, Ar(tetralin)-H), 6.99 (d, 1H, J = 8.0 Hz, Ar(tetralin)-H), 4.76 (s, 2H; N–CH_2), 2.80−2.77 (m, 2H; CH_2), 2.14−2.09 (m, 2H; CH_2), 1.99−1.94 ppm (m, 1H; CH_2), 1.87−1.81 ppm (m, 1H; CH_2), ^{13}C NMR (50 MHz, DMSO-d_6): δ = 176.5, 156.8, 147.3, 144.9, 138.4, 134.2, 129.9, 128.7, 127.1, 124.3, 114.4, 62.7, 41.3, 40.6, 39.3, 28.8, 18.9 ppm; Anal. Calcd. For $C_{19}H_{17}ClN_3O_4$: C, 64.95, H, 4.88, N, 11.96. Found: C, 64. 94, H, 4.89, N, 11.96.

2.2. In silico prediction

Determination of the relevant molecular descriptors for all synthesized compounds was assessed employing the following software packages: SwissADME (Swiss Institute of Bioin-formatics, Switzerland) [10] and PreADMET (East China University of Science and Technology, China) [11].

3. Results

3.1. Multiparametric optimization of molecular descriptors for the spirohydantoins derived from α-tetralone

For the last few years, drug discoveries have been established as the combination of experimental techniques and modern computational science. Different tools and techniques have been used for target identification, enrichment analysis and network algorithm. To date, several *in silico* bioinformatic methods have been developed and applied [12]. In the process of drug discovery, the relationship among drug structure, drug receptor affinity and drug bioavailability play a significant role in the viability of a drug candidate. Administered drug must possess not only intrinsic activity, but also favorable biopharmaceutical properties which allow drug molecules to cross membranes and attached to the corresponding receptors [13]. To develop drugs with a good therapeutic index, it is necessary to analyze the concepts of contents in Lipinski's rules, as well as the druglikeness parameters that make up the ADME (absorption, distribution, metabolism, and excretion) score. These parameters consider important factors of the behavior of a drug within the human body in order to favor a good therapy with great pharmacological potential and low toxicity. According to the Lipinski's rule compounds with good permeation and oral absorption possess molecular weight (MW) < 500 g/mol, log *P* < 5, hydrogen bond donor (HBD) < 5 and hydrogen bond acceptor (HBA) < 10 [14]. Molecules that are considered to have properties similar to standard drugs must not show more than one deviation from Lipinski's rule. Also, according to Veber's criteria, adequate oral bioavailability is achieved in molecules that have less than 10 rotatable bonds (nrb) and a topological polar surface area (TPSA) of less than 140 $Å^2$ [15]. According to the modified versions of these two concepts, in the case of compounds whose physicochemical properties satisfy the following ranges: 160 ≤ relative molecular mass ≤ 500; –0.4 ≤ WlogP < 5.6; 40 ≤ molar refractivity (MR) ≤ 130; 20 ≤ number of atoms (NA) ≤ 70 (Ghose's criteria) and WlogP ≤ 5.88, TPSA < 131.6 Å2 (Egan's criteria), there is a high probability of therapeutic effects [16].

Based on the values of molecular descriptors covered by these rules (Tables 1–2), it can be concluded that the examined imidazolidine-2,4-dione derivatives meet all the stated empirical criteria, i.e. meet the theoretical condition for adequate bioavailability and the appropriate pharmacological potential.

Table 1. Physico-chemical properties of the investigated compounds [10,11].

No.	*MW* [*g/mol*]	*NA*	*nrb*	*HBD*	*HBA*	*MR*	*TPSA* [A^2]
1	306.36	23	2	1	2	94.87	49.41
2	320.39	24	2	1	2	99.83	49.41
3	336.38	25	3	1	3	101.36	58.64
4	340.41	25	1	0	4	94.26	56.51
5	331.37	25	2	1	3	99.58	73.20
6	351.36	26	3	1	4	103.69	95.23

According to the unsubstituted compound **1**, the introduction of substituents at the *p*-position of the phenyl ring results in an increase in molecular weight. Based on the calculated value of the polar surface of the molecules (Table 1), it is expected that in *in vivo* conditions, the tested imidazolidine-

2,4-dione derivatives will show better intestinal absorption and passage through the blood-brain barrier. A moderate number of rotatable bonds that do not exceed 3 in all compounds, also contribute to the optimal passage of the studied compounds through the blood-brain barrier. According to the literature data, drugs that act on the central nervous system should have less than 8 rotatable bonds [16].

Table 2. Values of the partition coefficient of the investigated compounds [10,11].

No.	*$logP_{o/w}$ (XLOGP3)*	*$logP_{o/w}$ (WLOGP)*	*$logP_{o/w}$ (MLOGP)*
1	2.90	1.95	2.98
2	3.26	2.26	2.80
3	2.87	1.96	2.24
4	3.07	4.68	1.92
5	2.62	1.82	2.30
6	2.73	2.38	1.94

The data illustrated in Table 2, show that different values of the partition coefficient were obtained for the same compound, which is a consequence of a different mathematical algorithm for calculating this parameter within the software packages used. The highest values of the partition coefficient were obtained for compound **2**, which allows this compound to pass more successfully through the blood-brain barrier to passive diffusion as well as more successful binding to active sites at appropriate receptors, which is especially important for achieving the optimal concentration of drugs that act on the central nervous system [16]. High values of human intestinal absorption and plasma protein binding (Table 3) indicate good pharmacological potential of the investigated compounds.

Table 3. QSAR pharmacokinetic profiles of the investigated compounds related to absorption properties [10,11].

No.	*Human intestinal absorption*	*Human intestinal absorption, %*	*Plasma protein binding (%)*
1	High	95.67	100.00
2	High	95.77	99.41
3	High	95.77	98.81
4	High	96.15	92.51
5	High	96.34	99.63
6	High	96.09	94.55

3.2. A LSER analysis of the spirohydantoins derived from α-tetralone

To better understand nature of solute-solvent interactions, we applied the linear solvatation energy relationship concept developed by Kamlet, and Taft (equation 1). These quantitative concepts separate the influence of non-specific chemical interactions, including electrostatic effects (dipolarity/polarizability), from specific interactions, i.e. hydrogen-bonding, which concerns to the molecular

structure of a compound. The frequently employed simplified Kamlet–Taft equation applied to the UV/Vis absorption shift (ν_{max}) of a solute is presented by equation (1), where ν_{max0} is the solute property in a reference solvent, such as, a non-polar medium, α describes the HBD (hydrogen-bond donating) ability, β the HBA (hydrogen-bond accepting) ability, π^* the dipolarity/polarizability of the solvents and *a*, *b* and *s* are solvent-independent correlation coefficients that implies the contribution of various solvent effects to the UV-Vis absorption shift [7].

$$\nu_{max} = \nu_{max0} + a\alpha + b\beta + s\pi^* \quad (1)$$

To review this sensitivity and apart the individual solvation effects, the solvatochromic properties of these compounds were investigated in detail, and the coefficients of the individual interaction contributions were determined by using multiple correlation analysis.

*Table 4. Regression fits to solvatochromic parameters (**1**) and percentage contribution of solvatochromic parameters*

No.	ν_0 $(10^3 cm^{-1})$	*s* $(10^3 cm^{-1})$	*b* $(10^3 cm^{-1})$	*a* $(10^3 cm^{-1})$	R^a	s^b	F^c	$P\pi$ (%)	$P\beta$ (%)	$P\alpha$ (%)
1	45.49 (±1.84)	0.85 (±0.02)	–11.04 (±3.28)	12.11 (±2.30)	0.921	2.06	15	3.54	46	50.45
2	45.48 (±0.53)	–7.29 (±0.13)	–2.83 (±0.42)	8.38 (±0.69)	0.992	0.62	166	39.40	15.30	45.29
3	44.66 (±0.98)	–8.21 (±1.10)	–1.57 (±0.23)	6.54 (±1.29)	0.967	1.15	39	50.31	9.62	40.07
4	44.66 (±1.07)	–7.20 (±1.30)	–2.75 (±0.38)	8.39 (±1.14)	0.968	1.26	40	39.25	14.99	45.75
5	42.28 (±0.51)	–6.66 (±1.09)	1.45 (±0.39)	4.24 (±0.67)	0.982	0.604	74	53.93	11.74	34.33
6	39.27 (±0.93)	–0.53 (±0.03)	–1.24 (±0.02)	10.13 (±1.17)	0.972	1.12	46	4.45	10.42	85.13

[a]Correlation coefficient; [b]Standard error of the estimate; [c]Fisher's test.

Based on the results of multiple regressions presented in Table 4 we can conclude that the absorption frequencies of the investigated π-conjugated organic compounds in the selected solvent set, demonstrated satisfactory correlation with β, α, π^* parameters. The positive sign of the coefficient *s* in the case of compound **1** denotes the bathochromic shift with the increment of polarity/polarizability. Positive sign of the coefficient *a* indicates a hypsochromic shift of absorption maxima with the increase of solvent acidity, while negative sign of coefficient *b* (except in the case of **5**) implies bathochromic shift of absorption maxima with the increase of solvent basicity. The percentage contributions of the solvatochromic parameters (Table 4) demonstrate that solvatochromism in general is mostly affected by solvent acidity. Based on the values of the correlation coefficient *R* and other statistical parameters, it can be concluded that the selected equations are suitable for the analysis of the solvatochromism of the spirohydantoins derived from α-tetralone.

3.3. The correlation of solvent effects with the potential pharmacological activity of the spriohydantoins derived from α-tetralone

The influence of the solvent effects on the evaluated pharmacological activity of the imidazolidine-2,4-dione derivatives was first examined by plotting the calculated human intestinal absorption (HIA) values against the ratio a /|s| as a convenient measure of the relative contributions of the dominant modes of solvation (Equation 2 and Figure 1). The HIA values calculated by the PreADMET program were indicated as the percentage of a drug absorbed by the intestine (Table 3). The diagram illustrated in Figure 1 reveals that the investigated compounds behave differently, where the compound **5** possess the highest intestinal absorption, while the compound **1** possess the lowest absorption. As we can see from Figure 1, the influence of the CH_3 and OCH_3 groups attached to the *p*-position of the phenyl ring is the same. In other words, the electronic effects of both groups provide the same percentage of the intestinal absorption [17].

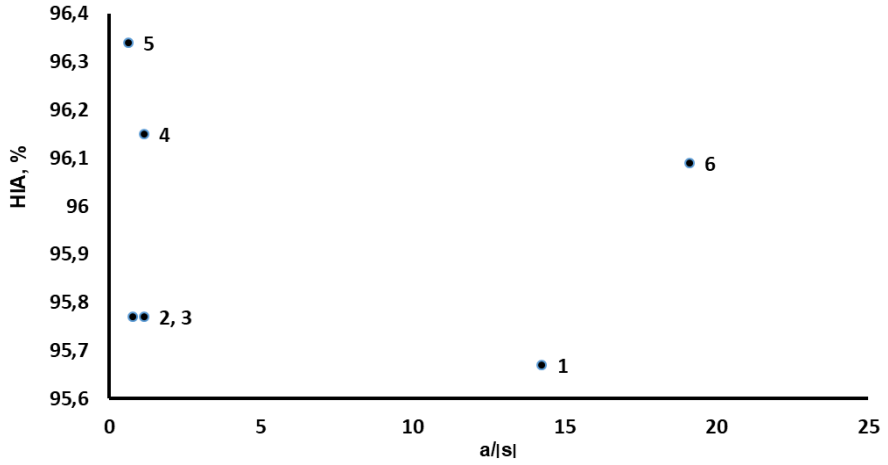

Figure 1. Correlation between the HIA values and the ratio of the contributions of the specific and non-specific solvent-solute interactions.

The improved correlation, which includes all of the investigated compounds, was derived through the additional inclusion of the resonance (σ_R) and inductive (σ_I) constants of substituents in *para* position of the phenyl ring (equation 2):

$$Abs = 95.88(\pm 0.10) - 0.02(\pm 0.01)a/|s| + 0.47(\pm 0.20)\sigma_I + 0.32(\pm 0.14)\sigma_R \quad (2)$$

$$(R = 0.955,\ s = 0.12,\ F = 7,\ n = 6)$$

It can be seen that Equation (2) has a meaning similar to the corresponding model of Abraham, when one realizes that the *a* and *s* coefficients refer to the hydrogen bond basicity and dipolarity/polarizability of the investigated compounds, respectively. The described concept of Abraham is constructed on the theoretical cavity model of solvent-solute interactions and successfully correlates different physicochemical properties of solutes. The Equation (2) shows that the hydrogen bond basicity of the investigated compounds decreases human intestinal absorption, whereas the dipolarity/polarizability enhances it [17].

4. Conclusion

In this work six new potentially pharmacologically active spirohydantoin derivatives were synthesized and completely structurally characterized using appropriate spectroscopic techniques. Prediction of potential pharmacological activity was preformed using different *in silico* methods and

empirical rules. The suitable correlations of the absorption maxima of the investigated spirohydantoins derived from α-tetralone with the solvent parameter set of Kamlet and Taft indicated that the selected model interpreted their LSER accurately. In the case, where both solvent and solute are hydrogen bond donors and acceptors, it was quite challenging to quantitatively estimate and separate the overall solvent effect into the contributions of specific and non-specific interactions. Nevertheless, such a separation provided further possibility to establish the structure-property relationships of the investigated molecules. The acquired models illustrated how various types of interactions and electronic effects of substituents on the phenyl ring influenced their pharmacological partitioning and binding to plasma proteins. The approach proposed in this work provided the means to analyze pharmacokinetic properties of hydantoin derivatives, not yet pharmacologically tested, which are challenging to determine experimentally.

5. Acknowledgement

This work was supported by the Ministry of Science, Technological Development and Innovation of the Republic of Serbia (Contract No. 451-03-66/2024-03/200287, 451-03-65/2024-03/200135 and 451-03-66/2024-03/200026).

6. References

[1] **Sousa Luis J. A., Barbosa Filho J. M., Bruno Freitas L., Almeida Medeiros I., Lima de Morais Soares L. C., Fernandes dos Santos A., Soares de Oliveira C.,** Filgueiras de Athayde-Filho P., Synthesis of new imidazolidin-2,4-dione and 2-thioxoimidazolidin-4-ones via *C*-phenylglycine derivatives, *Molecules* 15 (2010) 128–137.

[2] **Meusel M., Gütschow M.,** Recent developments in hydantoin chemistry. A review, *Organic Preparations and Procedures International: The New Journal for Organic Synthesis* 36 (2004) pp. 391–443.

[3] **Kumar V.,** Designed synthesis of diversely substituted hydantoins and hydantoin-based hybrid molecules: a personal account: *Synlett* 32 (2021) pp. 1897–1910.

[4] **Jaromin A., Czopek A., Parapini S., Basilico N., Misiak E., Gubernator J., Zagórska A.,** Synthesis and antiplasmodial activity of novel bioinspired imidazolidinedione derivatives, *Biomolecules* 11 (2021)1–12.

[5] **Verma S., Rani S.,** Synthesis, molecular docking and CNS activity of 5,5-diphenylimidazolidine- 2,4-dione derivatives, *Indian Journal of Chemistry* 62 (2023) 1151–1161.

[6] **Wang S., Ji L., Zhang D., Guo H., Wang Y., Li W.,** Synthesis and anti-inflammatory activity of 1-methylhydantoin cinnamoyl imides, *Molecules* 27 (2022) 8481–8493.

[7] **Lazić A., Mašulović A., Lađarević J., Valentić N.,** Assessing the pharmacological potential of selected xanthene derivatives, *Journal of Serbian Chemical Society* 88 (2023) 811–824.

[8] **Naydenova E., Pencheva N., Popova J., Stoyanov N., Lazarova M., Aleksiev B.**, Aminoderivatives of cycloalkanespirohydantoins: synthesis and biological activity, *Farmaco* 57 (2002) 189–194.

[9] **Suzuki H., Kneller M. B. B., Rock D. A., Jones J. P., Trager W. F., Rettie A. E.,** Active-site characteristics of CYP2C19 and CYP2C9 probed with hydantoin and barbiturate inhibitors, *Archives of Biochemistry and Biophysics* 429 (2004) 1–15.

[10] *** http://www.swissadme.ch/. Accessed 10.02.2024.

[11] *** https://preadmet.bmdrc.kr/. Accessed 10.02.2024.

[12] **Yin L., Zheng L., Xu L., Dong D., Han X., Zaho Y., Xu Y., Peng J.,** *In silico* prediction of drug targets, biological activities, signal pathways and regulating networks of dioscin based on bioinformatics, *BMC Complementarary and Alternative Medicine* 15 (2015) 41–53.

[13] **Abdulrahman L. K., Al-Mously M. M., Al-Mosuli M. L., Al-Azzawii K. K.,** The biological activity of 5,5'-imidazolidine-2,4-dione derivatives, *International Journal of Pharmacy and Pharmaceutical Sciences* 5 (2013) 494–504.

[14] **Gimenez B. G., Santos M. S., Ferrarini M., Fernandes J. P. S.,** Evaluation of blockbuster drugs under the Rule of five, *Pharmazie* 65 (2010) 148–152.

[15] **Veber D. F., Johnson S. R., Cheng H.-Y., Smith B. R., Ward K. W., Kopple K. D.,** Molecular properties that influence the oral bioavailability of drug candidates, *Journal of Medicinal Chemistry* 45 (2002) 2615–2623.

[16] **Lazić A., Mandić Ž., Uščumlić G., Trišović N.,** Dizajn, sinteza i evaluacija farmakokinetički relevantnih svojstava novih spirohidantoina izvedenih iz *β*-tetralona, *Hemijska Industrija* 73 (2019) 79–92.

[17] **Hmuda S. F., Banjac N. R., Trišović N. P., Božić B. Đ., Valentić N. V, Gordana U. S.,** Solvent effects on the absorption spectra of potentially pharmacologically active 5-alkyl-5-arylhydantoins-a structure-property relationship study, *Journal of the Serbian Chemical Society* 78 (2013) 628–635.